Statistical Coulomb interactions in multi-beam SEM

Stopka, Jan; Kruit, Pieter

DOI
10.1142/S0217751X19420211

Publication date
2019

Document Version
Accepted author manuscript

Published in
International Journal of Modern Physics A

Statistical Coulomb Interactions in Multi-Beam SEM

Jan Stopka

Institute of Scientific Instruments, Czech Academy of Science, Královopolská 147
Brno, 612 64, Czech Republic
jstopka@isibrno.cz

Pieter Kruit

Dept. Imaging Physics, Delft University of Technology, Lorentzweg 1,
Delft, 2628CJ, The Netherlands
p.kruit@tudelft.nl

Statistical Coulomb interactions in conventional scanning electron microscopy mostly affect the probe size via energy spread and virtual source broadening in the emitter vicinity. However, in a multi-beam probe forming system such as a multi-beam Scanning Electron Microscopes (MBSEM), the trajectory displacement due to interactions in the whole column can give a contribution to the final probe size. For single-beam systems, this can be expressed using approximate formulae for the total trajectory displacement in a beam segment (Jansen's theory) or by integrating contributions of infinitesimally thin beam slices (the slice method). We build on Jansen's theory of statistical Coulomb interactions and develop formulae for the trajectory displacement in a multi-beam system. We also develop a more precise semi-analytical result using the slice method. We compare both approaches with a Monte-Carlo simulation and show a good agreement with the results of the slice method. Finally, we discuss the implications of our results for the optical design of multi-beam SEM. In a multi-beam with probe size dominated by Coulomb interactions, an increase in the number of beamlets does not necessarily provide an increase of throughput, because the probe size is limited by the total current. Furthermore, we disprove the notion of "the fewer crossovers – the less Coulomb interactions" by showing the quadratic dependence of trajectory displacement on segment length.

Keywords: Coulomb interactions; trajectory displacement; multi-beam SEM; electron optics; slice method.

1. Introduction

Charged particles, unlike photons, interact with each other by the Coulomb repulsion. The Coulomb interaction in charged particle beams can be described as a combination of three effects. The space charge effect is the repulsion caused by the averaged charge density of the beam. The Boerch effect and the trajectory displacement are statistical effects caused by the stochastic nature of the particle beam. The former describes longitudinal acceleration or deceleration of individual particles which manifests itself as energy broadening of the

beam. The latter is a transverse effect and, as the name suggests, describes the displacement of the particle trajectory.[1]

An analytic solution to the many body problem of Coulomb interactions in particle beam is not feasible. An exhausting description starting at two particle dynamic and ending with an approximate but general formula for Coulomb interaction effects using macroscopic beam parameters was given by Jansen.[2]

Although these formulae allow calculation of Coulomb interactions for a wide range of system parameters such as current, energy or beam dimensions, they are derived for a single particle beam of cylindrical or conical shape. There are, however, more complicated systems such as projection- or multi-beam electron lithography machines[3,4] and multi-beam scanning electron microscopes,[5] which can be limited by statistical Coulomb interactions.

Multi-beam systems have a very different beam geometry than single beam systems and a revision of the formulae is therefore needed in order to be able to estimate statistical Coulomb interactions in such a system. In the type of multi-beam system that is the subject of this study, the beam from a single electron source is split in multiple beams, typically tens to hundreds.[6–9] An array of miniature lenses creates an array of source images, which are subsequently demagnified and imaged onto a specimen using one or more macro-lenses. In the example of Ref. 8, this demagnification is performed by a standard SEM column.

In the following sections we briefly introduce Jansen's theory of trajectory displacement and we modify the formulae to describe a trajectory displacement in multi-beam systems.

2. Theory of trajectory displacement

In this section we give a brief introduction into the analytic model of trajectory displacement (TD) as derived by Jansen.[2,10] For simplicity we assume that the beam is divided into several segments by thin optical components (lenses). The individual contributions from the segments can then be combined together to obtain the total TD of the system.

The analytic model of statistical Coulomb interactions is based on the so called two-particle interaction model. The two-particle model assumes the current to be small enough that the Coulomb interactions between the particles are rare and the scattering events can therefore be treated as uncorrelated. Full description of this model is out of scope of this section and for detailed information see Ref. 2.

There are a few important parameters defining the geometry of the beam segment. There is the length of the segment L, the distance from the start of the segment to the beam crossover L_c and the distance from the start of the segment to the Gaussian image plane L_i (for a multi-beam L_c and L_i are generally different). It is useful to normalize the two distances by the segment length and therefore obtain two dimensionless parameters

$$S_c = \frac{L_c}{L}, \qquad S_i = \frac{L_i}{L}. \tag{1}$$

The lateral geometry of the beam segment is described by the beam radius of the crossover r_c and by the semi-angle of the beam envelope α_0. From those we can construct

the so called characteristic beam diameter

$$K = \frac{\alpha_0 L}{2r_c}. \tag{2}$$

The beam itself is also defined by the total current I and potential V.

A general formula covering all meaningful settings of the system is not known, and so it is necessary to interpolate between different regimes which describe asymptotic approximations. We limit ourselves to relatively low current, or more specifically low dimensionless particle density. The dimensionless particle density is given by a ratio between the average kinetic energy in the frame of reference moving with the beam and the potential energy between a pair of particles with average axial separation. It can be expressed as

$$\lambda^* = \frac{e^2\lambda/4\pi\varepsilon_0}{m\left(\alpha_0 v_z\right)^2} = \sqrt{\frac{m_e}{2^7\pi^2\varepsilon_0^2 e}} \cdot \frac{I}{\alpha_0^2 V^{3/2}}. \tag{3}$$

For values of $I \approx 100\,\mathrm{nA}$, $V \approx 5\,\mathrm{kV}$ and $\alpha_0 \approx 0.1\,\mathrm{mrad}$ we have $\lambda^* \approx 0.2$. Typically we deal with lower currents, higher energies and larger semi-angles, so $\lambda^* \ll 1$, therefore the mutual potential energy is much less than the transverse kinetic energy and thus the collissions are weak and we can consider only Holtzmark and Pencil beam regimes. The Holtzmark regime describes the asymptotic case where the charge is uniformly distributed in the whole 3D space. Pencil-beam, on the other hand, describes the case where the distance of the particles to the optical axis is much less than their longitudinal spacing. There are formulae for trajectory displacement in these regimes:[2]

$$FW_{50,HT} = 2.35 \cdot S_{HT}(S_c, S_i, K) \cdot \frac{L^{2/3} I^{2/3}}{\alpha_0^{4/3} V^{4/3}}, \tag{4}$$

$$FW_{50,PT} = 2.16 \cdot 10^{30} \cdot S_{PT}(S_c, S_i, K) \cdot \frac{L^3 \alpha_0 I^3}{V^{5/2}} \tag{5}$$

The constants are in SI units. The functions S_{HT} and S_{PT} are specified by Jansen.[10]

Usually, we are not entirely in one of those regimes and therefore it is necessary to take both contributions into account and interpolate between them using the power-sum rule:[1]

$$FW_{50} = \left(FW_{50,HT}^{-6/7} + FW_{50,PT}^{-6/7}\right)^{-7/6} \tag{6}$$

3. Trajectory displacement in a multi-beam system

In a multi-beam system, the aim is to project an array of (virtual) sources into the image plane. In our case we assume a square array of $N \times N$ sources, but the concept can be easily extended to other geometries as well. Ideally, all beamlets are focused in this plane. However, this is challenging to achieve due to geometrical aberrations of the lenses. One way to minimize the effect of geometrical aberrations is to position all the lenses either in an image plane where all beamlets are focused or in the common crossover plane.[11] Such a geometry can be treated as a series of segments described in figure 1 or its mirror counterpart.

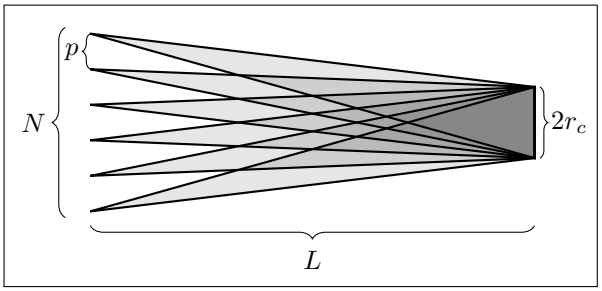

Figure 1. Multi-beam segment section. The segment is described by four parameters: N the number of beamlets in one row/column, p the pitch, L the length of the segment and r_c the field radius in the common crossover.

For such a segment we have $S_i = 0$ and $S_c = 1$. The formulae (4) and (5) are derived for a single beam segment. In order to use them for the multi-beam segment, we approximate the multi-beam field by a single fully filled segment. This approximation is valid for a sufficiently large number of beamlets, but it would fail for a system with only a few beamlets. For a square array of N^2 beamlets with a pitch p, this approximation replaces the square array by a circle of the same area. The radius of the circle is thus $r_1 = \frac{Np}{\sqrt{\pi}}$. Since the crossover is at the end of the segment, this radius is related to the semi-angle $\alpha_0 = \frac{r_1}{L} = \frac{Np}{\sqrt{\pi}L}$. This gives the characteristic beam diameter $K = \frac{Np}{2\sqrt{\pi}r_c}$.

With this setting, the functions S_{HT} and S_{PT} take the form

$$S_{HT} = 3 \cdot \frac{1 + \frac{4}{3}K - (1+2K)^{2/3}}{2K^{2/3}}, \tag{7}$$

$$S_{PT} = \frac{3+2K}{K}. \tag{8}$$

Finally we get for trajectory displacement in multi-beam segment for Holtzmark and pencil-beam regime respectively:

$$\begin{aligned} FW_{50,HT} =& 7.41 \frac{L^2 I^{2/3}}{N p r_c^{1/3} V^{4/3}} \cdot \\ & \cdot \left(1 + \frac{3}{4K} - \frac{3}{4K^{1/3}} \left(2 + \frac{1}{K}\right)^{2/3}\right), \end{aligned} \tag{9}$$

$$FW_{50,PT} = 2.44 \cdot 10^{30} \cdot \frac{N p L^2 I^3}{V^{5/2}} \left(1 + \frac{3}{2K}\right) \tag{10}$$

4. Slice method

The above mentioned formulae (9) and (10) work best for a segment operating under one particular regime (either Holtzmark or pencil beam). For an intermediate regime, the interpolation formula (6) seem to give a good approximation for single beam segments. However, this may not be the case for multi-beam segments and we should check this carefully. An alternative for interpolating between between the results of the purely Holtzmark and

pencil-beam regime as in equation 6, is to use the slice method.[12] This consists of calculating the total TD contribution from all regimes in thin cylindrical slices across the segment length and integrating these total TD contributions to obtain the TD in the segment. The differential contributions for Holtzmark and pencil beam regime in a thin slice of thickness Δz can be expressed[2] as

$$\frac{\Delta FW_{50,HT}}{\Delta z} = C_H \frac{I^{2/3}}{V^{4/3} r_c^{4/3}} \frac{z - z_i}{\left(1 + \frac{\alpha_0 |z - z_c|}{r_c}\right)^{4/3}}, \tag{11}$$

$$\frac{\Delta FW_{50,PT}}{\Delta z} = C_P \frac{I^3 r_c}{V^{5/2}} (z - z_i) \left(1 + \frac{\alpha_0 |z - z_c|}{r_c}\right) \tag{12}$$

with $C_H = 1.393$ and $C_P = 2.593 \cdot 10^{31}$ in SI units.

We can combine both regimes with the addition rule

$$\Delta FW_{50} = \left(\Delta FW_{50,HT}^{-6/7} + \Delta FW_{50,PT}^{-6/7}\right)^{-7/6}. \tag{13}$$

The trajectory displacement can then be calculated as

$$FW_{50} = \left| \int_0^L \frac{\Delta FW_{50}}{\Delta z} \, \mathrm{d}z \right|. \tag{14}$$

The direct integration of total differential contributions using the slice method has the potential of being much more precise than the power sum of the total trajectory displacements for the two regimes. On the other hand, the integral can not be expressed analytically, so it is not that straightforward to see dependencies on individual parameters of the system.

5. Boerch effect in a multi-beam system

In a single beam probe forming system it is often not the trajectory displacement that is of most concern, but rather the Boersch effect – broadening of the energy distribution due to statistical Coulomb interactions.

The reason is the chromatic aberration of the system, which is typically dominant over the trajectory displacement.

However, this is not the case for a multi-beam system where an array of focused spots is imaged because with the same beamlet semi-angles and lens excitations as in single-beam system we have much larger total current.

To get an estimate of the Boerch effect for a multi-beam, we use expressions for a segment geometry with a narrow crossover:

$$\frac{\Delta E_{FW_{50,H}}}{E} = 0.891 \frac{m_e^{1/3}}{\varepsilon_0} \frac{I^{2/3}}{r_c^{1/3} \alpha_0 V^{4/3}}, \tag{15}$$

$$\frac{\Delta E_{FW_{50,P}}}{E} = 0.642 \frac{m_e}{\varepsilon_0 e^2} \frac{I^2 L}{V^2}, \tag{16}$$

$$\frac{\Delta E_{50}}{E} = \frac{1}{E} \left(\Delta E_{50,H}^{-4} + \Delta E_{50,P}^{-4}\right)^{-1/4} \tag{17}$$

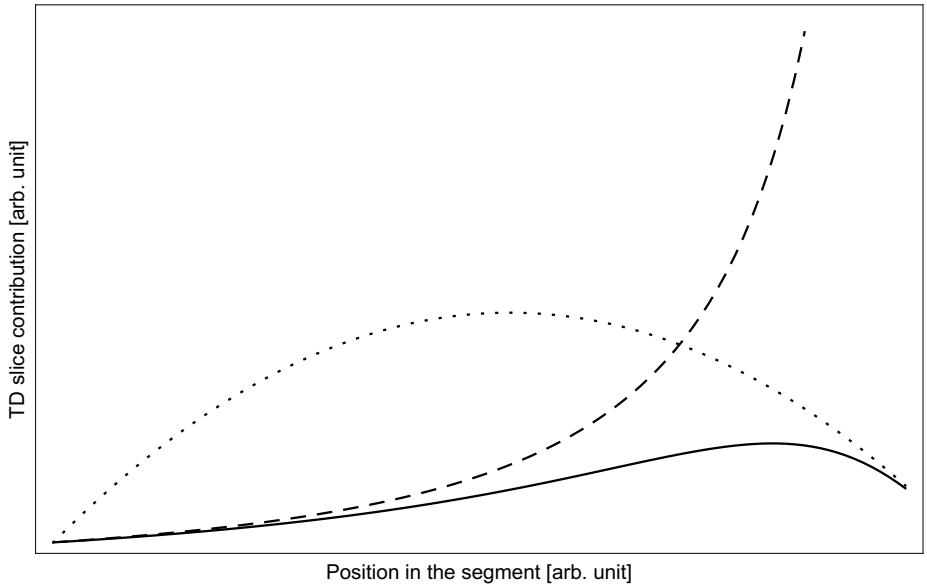

Figure 2. Differential contribution to trajectory displacement for Holtzmark (dashed) and pencil-beam (dotted) regimes and the corresponding power-sum (solid) as functions of position within the segment. A transition from Holtzmark to pencil-beam regime across the segment is clearly visible.

This expression gives an energy spread of about $0.05\,\mathrm{eV}$ for a typical setting with ~ 100 beamlets, $500\,\mathrm{pA}$ beamlet current, $5\,\mathrm{keV}$ energy, $0.1\,\mathrm{mrad}$ semi-angle, $100\,\mu\mathrm{m}$ crossover radius and $500\,\mathrm{mm}$ segment length. This is much lower than the energy spread of the emitter ($\sim 0.8\,\mathrm{eV}$ for a Schottky emitter), so the Boerch effect in multi-beam can be in our case neglected.

6. Monte Carlo simulation

In order to validate our formulae for the trajectory displacement in a multi-beam system we performed a Monte Carlo simulation using the software General Particle Tracer.[13] Experimental verification of Monte Carlo simulation of statistical Coulomb interactions in multi-beam system was performed in Ref. 14.

The layout of the simulation follows the segment geometry depicted on figure 1. A large number of particles ($n = 4 \cdot 10^5$) is launched from a square array of N^2 point sources towards a common crossover. The temporal distribution of the particles is uniform. The angular distribution within each beamlet is also uniform.

Since the common crossover is not in the image plane, in order to determine the trajectory displacement it is necessary to back-project the particles from the common crossover to the starting plane. There we see a clear blur of the originally point-like source. In order to estimate the FW_{50} of the spot we first determine its center as a point $(\mathrm{med}\, x, \mathrm{med}\, y)$. Then for each particle we calculate its distance to this center. Double the median of these distances is our FW_{50} estimate. This metric is simple, but robust, reliable and resilient to

Beamlet current	$I_b\,[\mathrm{nA}]$	0.1, 0.2, **0.3**, 0.45, 0.65, 0.85, 1.0
Energy	$V\,[\mathrm{keV}]$	3, 5, 7, 9, **11**, 13, 15, 17, 20
Segment length	$L\,[\mathrm{mm}]$	100, 150, 200, 250, 300, 350, 400, **450**
Semi-angle	$\alpha\,[\mathrm{mrad}]$	0.06, 0.09, 0.13, **0.20**, 0.30, 0.45, 0.68
Pitch	$p\,[\mu\mathrm{m}]$	20, 40, 60, **80**, 100, 130, 160

outliers.

A base setting was chosen and for each of the system parameters a number of runs was performed to deduce the dependence on each parameter. The set of parameters is described in table 1 with the base setting typed in bold. For all runs the beamlets were arranged in a square array of 14×14 beamlets.

7. Comparison of the methods

The results of the Monte Carlo simulation can be compared with the theoretical calculation using the integral formulae (6), (9), (10) and the slice method using (11), (12), (13). The comparison is shown in figure 3.

The integral formula gives TD in the correct order of magnitude and some trends such as the quadratic dependence on segment length or current and voltage dependence are predicted fairly well. However, the integral formula fails to accurately describe dependence on the cross-over radius due to the transition between Holtzmark and pencil-beam regime.

On the other hand, the slice method provides an elegant solution to the problem with the transition. We can see that the slice method fits the Monte-Carlo simulation very well and even predicts correctly the dependence on the common-crossover radius.

8. Dependence on beamlet position

The theory and expressions developed so far are only valid for the central beamlet. The effect of trajectory displacement is weaker for beamlets further away from the axis. We can predict the trajectory displacement in the outermost (corner) beamlet by the following consideration. Let us think about the field as four congruent, touching fields with each one quarter of the current. From the two particle interaction approximation we can deduce that when part of the field is rotated around a certain beamlet, the trajectory displacement in the beamlet does not change. This lets us "unwrap" the four components around the corner beamlet effectively making it the central beamlet of a different multi-beam setup. Thus the trajectory displacement of the corner beamlet can be calculated using the same formulae as for the center beamlet, but with a transformation $I_b \longmapsto I_b/4$ and $N \longmapsto 2N$, at the same pitch. The transformation is explained in figure 4.

The ratio between the trajectory displacement for the innermost and outermost beamlet depends on N. For values of about $N \sim 10$ it is less than 2, so the trajectory displacements for all beamlets are comparable. To obtain the trajectory displacement for any other beamlet we can use linear interpolation of the two (dependent on distance of the beamlet from the axis).

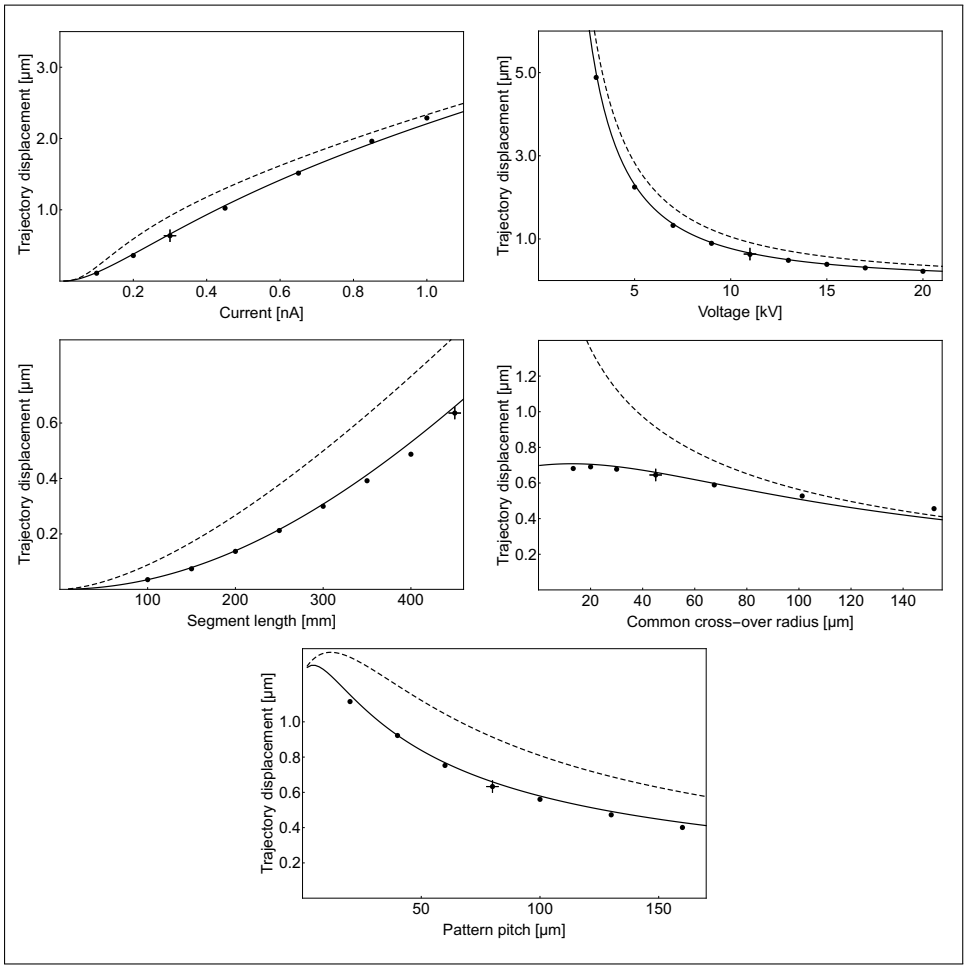

Figure 3. Comparison of analytical formulae for the total TD (dashed line), the slice method calculation (solid line) and Monte-Carlo simulation (dots) with base setting emphasized (a cross). Dependence of trajectory displacement on various parameters of the system.

Validity of this prediction was tested by a Monte-Carlo simulation described in the previous section. The transformed analytical formula does not describe the trajectory displacement of the outer beamlet very precisely (off by a factor of 0.7). However, the slice method using transformed formulae fits the simulated data very well.

9. Implications for design of MBSEM

The studied behavior of trajectory displacement has important implications for the design of electron optics of TD limited systems such as the MBSEM. The first is the obvious conclusion that a shorter system is better, similar to all systems with trajectory displacement. The second is that the quadratic dependence of TD on segment length suggests that

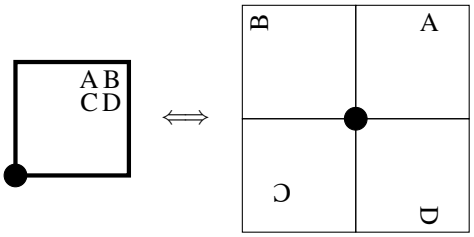

Figure 4. Unwrapping the field around the corner beamlet moves it into the center of the field. The TD for the corner beamlet can be then calculated using the formula for the central one with a transformation $I_b \longmapsto I_b/4$ and $N \longmapsto 2N$.

having a system with multiple shorter segments can reduce the effect of trajectory displacement. A Monte Carlo simulation verified this behavior. There are, of course, limitations, as multiple shorter segments require more lenses and thus may introduce larger geometrical aberrations. Let us return to the question of how to add the contributions from different segments. For a single beam system with the image plane in the cross-over ($S_c = S_i$), the displacement contributions from both sides of the cross-over add up and there are arguments to add the contributions from subsequent sections linearly as well if the individual collisions are incomplete throughout the column. In the multi-beam configuration, however, displacements on one side of the cross-over may compensate displacements at the other side. Further study of this effect is underway.

Another important remark concerns the number of beamlets in a MBSEM. The throughput of a system is roughly given by the total current of the multi-beam. For low number of beamlets or low currents, the probe size is given by geometrical aberrations of the system. Increase in number of beamlets thus gives higher total current with the same probe size. However, for high number of beamlets or high beamlet currents the probe size is dominated by trajectory displacement and increase in number of beamlets does not improve the throughput anymore, since in order to preserve the probe size it is necessary to decrease the beamlet current.

Last but not least it is worth noting that the TD in a segment manifests itself in the image plane of the segment and effectively behaves as an enlargement of the source size. For large currents it is therefore advantageous to increase the demagnification of the system, as the TD is demagnified along with the virtual source. When we combine this argument with the above analysis on the number of beamlets, it may turn out that a larger number of beamlets even has a disadvantage as compared to an intermediate number: a larger N leads to a smaller pitch in the object plane of the segment. A large demagnification may then lead to an unacceptably small pitch at the specimen.

10. Conclusions

This article studied the trajectory displacement in a simplified segment of a multi-beam system. We approximated the multi-beam by a fully-filled circular single-beam of the same dimensions to use the well-known expressions for trajectory displacement in a single-beam

segment.

This allowed us to derive an analytic expression for the total trajectory displacement in a multi-beam segment as well as a differential contribution from a thin slice of the segment. Both approaches were compared with a Monte Carlo simulation of the multi-beam segment.

While the Monte Carlo method gives most reliable results, it is very time consuming and it gives no insight into the overall behaviour of the trajectory displacement. We have shown that the analytic expressions for trajectory displacement fail to give accurate estimates for a segment with a transition from one regime to the other. On the other hand, the slice method is a fast and reliable way to accurately estimate the trajectory displacement even for configurations with such a transition.

11. Acknowledgements

The research was supported by the TA CR (TE01020118), the MEYS CR (LO1212), its infrastructure by the MEYS CR and the EC (CZ.1.05/2.1.0 0/01.0 017) and by the CAS (RVO:68081731). We would like to thank Bohuslav Sed'a, Eric Kieft and Ali Mohammadi-Gheidari of Thermo Fisher Scientific and Tomáš Radlička of Institute of Scientific Inrtruments of the CAS for their contribution and helpful remarks. J. S. thanks Bas van der Geer, the author of General Particle Tracer, for his help with the software.

Bibliography

1. P. Kruit and G. H. Jansen, Space charge and statistical coulomb effects, in *Handbook of charged particle optics*, ed. J. Orloff (CRC Press, Boca Raton, c2009) pp. 341–389, 2nd edn.
2. G. H. Jansen, *Coulomb interactions in particle beams* (Academic Press, Boston, c1990).
3. J. A. Liddle *et al.*, *Journal of Vacuum Science & Technology B* **19** (2001), doi:10.1116/1.1359174.
4. M. McCord, S. Kojima, P. Petric, A. Brodie and J. Sun, *Journal of Vacuum Science & Technology B* **28**, C6C1 (2010), doi:10.1116/1.3505130.
5. A. Eberle *et al.*, *Journal of Microscopy* **259**, 114 (2015), doi:10.1111/jmi.12224.
6. Y. Zhang and P. Kruit, *Physics Procedia* **1**, 553 (2008), doi:10.1116/1.588661.
7. A. Mohammadi-Gheidari, *196 Beams in a Scanning Electron Microscope* (Delft University of Technology, Delft, 2013).
8. A. Mohammadi-Gheidari and P. Kruit, *Nuclear Instruments and Methods in Physics Research Section A: Accelerators, Spectrometers, Detectors and Associated Equipment* **645**, 60 (2011), doi:10.1016/j.nima.2010.12.090.
9. A. Mohammadi-Gheidari, C. W. Hagen and P. Kruit, *Journal of Vacuum Science & Technology B* **28**, C6G5 (2010), doi:10.1116/1.3498749.
10. G. H. Jansen, *Journal of Applied Physics* **84**, 4549 (1998-10-15), doi:10.1063/1.368681.
11. Y. Ren and P. Kruit, *Journal of Vacuum Science & Technology B* **34** (2016), doi:10.1116/1.4966216.
12. X. R. Jiang, J. E. Barth and P. Kruit, *Journal of Vacuum Science & Technology B: Microelectronics and Nanometer Structures Processing, Measurement, and Phenomena* **14** (1998), doi:10.1116/1.588661.
13. Pulsar Physics, General Particle Tracer, `http://www.pulsar.nl/gpt`.
14. M. Mankos, A. Sagle, S. T. Coyle and A. Fernandez, *Journal of Vacuum Science & Technology B* **19** (2001), doi:10.1116/1.1420200.